doi: 10.4149/gpb_2025030

Curcumin-chitosan microspheres inhibit epithelial cell PANoptosis: analysis of key PANoptosis gene distribution *via* single-cell RNA sequencing and *in vivo* validation in ulcerative colitis mice

Xinyou Pan[1], Qiaohong Zhu[2], Yanru Xiang[2], Jiaqi Liu[3], Chengdong Yu[2] and Guodong Huang[2]

[1] *Department of Traditional Chinese Medicine, The First Affiliated Hospital, Jiangxi Medical College, Nanchang University, Nanchang, Jiangxi, China*
[2] *Anorectal Department of Integrated Traditional Chinese and Western Medicine, The First Affiliated Hospital, Jiangxi Medical College, Nanchang University, Nanchang, Jiangxi, China*
[3] *Department of Ophthalmology, The First Affiliated Hospital, Jiangxi Medical College, Nanchang University, Nanchang, Jiangxi, China*

Abstract. Our previous research has confirmed that curcumin ameliorates pathology of ulcerative colitis (UC) in mice. PANoptosis is closely associated with UC; however, whether curcumin-chitosan microspheres (CCM) alleviate UC by modulating intestinal epithelial cell PANoptosis remains unreported. Here, CCM significantly inhibited UC-induced damage to colon tissue, as evidenced by increased colon length and reduced DAI score, as well as lower concentrations of inflammatory factors (IL-18 and IL-1β). CCM also suppressed expression of tight junction marker ZO-1 and PANoptosis marker NLRP12 induced by UC in colon tissue, and we observed the co-localization of ZO-1 and NLRP12. scRNA-seq revealed eight subpopulations of intestinal epithelial cells and crypt top colonocytes had the highest PANoptosis score. Expression of PANoptosis-related markers (ASC, NLRP3, NLRP12, and caspase-8) was downregulated after CCM treatment in scRNA-seq data. Different concentrations of CCM (20, 40, 80 μM) did not alter the cell viability of Caco-2 cells, but significantly reduced LPS-induced death and the elevation of inflammatory factors. LPS provoked protein expression of PANoptosis-related markers in Caco-2 cells, but this effect was reversed by CCM. In conclusion, CCM ameliorate UC by inhibiting epithelial cell PANoptosis, indicating that CCM is a promising therapeutic strategy against UC from the prospective of epithelial cell PANoptosis.

Key words: Ulcerative colitis — Curcumin-chitosan microspheres — PANoptosis — scRNA-seq — Intestinal epithelial cells

Introduction

Ulcerative colitis (UC) is a complex and elusive chronic inflammatory bowel disease that often significantly affects the quality of life of patients. UC involves not only persistent inflammation of the intestines but can also lead to a variety of symptoms, including abdominal pain, diarrhea, and weight loss, placing a heavy physical and mental burden on patients (Feuerstein et al. 2019). The incidence of UC was 24.3 *per* 100,000 person-years which has attracted widespread attention in recent years (Molodecky et al. 2012). Research data shows that the incidence of UC has been showing a rising trend year by year, particularly evident among young people and certain high-risk groups (Xu et al. 2023). This rising

Correspondence to: Guodong Huang, Anorectal Department of Integrated Traditional Chinese and Western Medicine, The First Affiliated Hospital, Jiangxi Medical College, Nanchang University, Nanchang, Jiangxi, China
E-mail: hgddr233011@sina.com

trend not only reflects the impact of the disease on specific populations but also highlights the urgent need for response measures in the field of public health. Therefore, understanding the pathogenesis of UC is crucial not only for patients but also provides important reference for healthcare professionals and public health policymakers to develop more effective prevention and treatment strategies.

Our preliminary research has substantiated the ameliorative effects of curcumin plus Soy oligosaccharides in UC (Huang et al. 2017). Curcumin possesses anti-inflammatory, antioxidant, and apoptosis-regulating properties and can be used for disease treatment (Nelson et al. 2017). Consistent with our findings, several studies have elucidated the therapeutic effects of curcumin complexes in UC. For instance, in this placebo-controlled trial, Ben-Horin et al. has demonstrated that the curcumin-qingdai combination can alleviate symptoms of active UC patients. Nanohybrid of CCM-CoFe Prussian blue analogs enables remission the symptoms of UC mice (Yao et al. 2023). In a similar manner, lipid-based nanocarriers functionalized with hyaluronic acid have been shown to markedly improve the physicochemical stability and anti-inflammatory activity of curcumin (Feng et al. 2025a) in colitis mice (Feng et al. 2025b). However, the widespread application of curcumin as a treatment for UC is hindered by the lack of a drug delivery system that can provide sustained release of curcumin over a long period while maintaining its bioactive properties. To address this issue, we previously prepared curcumin-chitosan microspheres (CCM) using chitosan, a biopolymer with sustained release characteristics, as a carrier (Yu et al. 2019). Chitosan microspheres serve as a drug delivery system that enhances the stability and bioavailability of the drug. We have officially confirmed that CCM is more effective than the use of curcumin alone for the treatment of UC (Yu et al. 2022). However, the molecular mechanism by which CCM improves UC is still unclear.

PANoptosis is a unique mode of inflammatory cell death that involves the interaction between pyroptosis, apoptosis, and necrosis, and can be mediated by a multifaceted PANoptosome complex assembled by integrating components from other cell death modes (Sun et al. 2024). An increasing number of studies indicate that PANoptosis plays an important role in the progression of UC disease (Wang et al. 2023; Lu et al. 2024). Epithelial cell PANoptosis is receiving increasing attention, as this process not only affects the health and function of blood vessels but may also be closely related to the occurrence and development of various diseases, for example, epithelial cell PANoptosis activated by mitochondrial fission and thus accelerating UC progression (Ye et al. 2024). Intestinal epithelial cells PANoptosis induced by Salmonella effector SopF involved in systemic infection (Yuan et al. 2023). Intestinal epithelial cells play a vital role in maintaining normal intestinal function; they are not only involved in the absorption and transportation of substances but also serve as a crucial barrier to protect the intestine from harmful substances. Given the potential modulatory effects of curcumin in various biological processes, investigating its impact on epithelial cell PANoptosis is of paramount importance. However, the role of epithelial cell PANoptosis in UC has not been fully uncovered, and it is also unknown whether CCM can exert its beneficial effects by regulating intestinal epithelial cell PANoptosis.

The specific focus of this research is the regulatory effect of CCM on intestinal epithelial cell PANoptosis in UC. In this study, we employ single-cell RNA sequencing (scRNA-seq), cytotoxicity assessments, and various biological detection techniques to evaluate the influence of CCM on epithelial cell PANoptosis. This research endeavors to fill the existing knowledge gaps regarding the modulation of epithelial cell PANoptosis by CCM and provide theoretical support and experimental evidence for clinical treatment of relevant diseases.

Materials and Methods

CCM preparation

CCM were prepared using an emulsified cross-linking method. Briefly, 300 mg of chitosan (#C105799, Aladdin) was dissolved in 20 ml of 3% acetic acid at 40°C to obtain a 15 mg/ml chitosan solution, followed by degassing and filtration through a 0.45 μm membrane. Separately, 50 mg of curcumin was dissolved in 1 ml of anhydrous ethanol to obtain a 10 mg/ml curcumin solution. Then, 4 ml of the chitosan solution was mixed with 1 ml of the curcumin solution and stirred thoroughly, maintaining a curcumin-to-chitosan molar ratio of 1:2. The resulting aqueous phase was added dropwise into 40 ml of liquid paraffin containing 2 ml of SP80 (5%) under continuous stirring at 600 rpm to form a stable water-in-oil (W/O) emulsion, which was maintained for 2 hours. Subsequently, 5 ml of sodium tripolyphosphate solution (1.4 mg/ml, prepared by dissolving 14 mg of sodium tripolyphosphate in 10 ml deionized water and filtering through a 0.45 μm membrane) was added into the emulsion at a rate of 5 ml/min using a needleless syringe while stirring, allowing crosslinking to proceed for 1 hour. This crosslinking step was repeated once more, totaling 10 ml of sodium tripolyphosphate solution and 2 hours of crosslinking. The resulting microspheres were collected by centrifugation at 8000 rpm for 10 minutes and washed three times with ethanol to remove unreacted curcumin. The final product was pre-frozen at −80°C for 2 hours and lyophilized under vacuum for 12 hours to obtain dry, fluffy CCM powder.

Scanning electron microscope (SEM)

The surface morphology of CCM was observed using a SEM (QUANTA 250, FEI, USA). First, the CCM samples were subjected to vacuum freeze-drying for 24 hours using a lyophilizer to obtain dry microspheres. A small amount of conductive adhesive was applied to the SEM sample stub using a toothpick, ensuring that the adhesive area was slightly smaller than the sample base. The dried microspheres were carefully placed onto the adhesive using tweezers, with the surface of interest facing upward. After the conductive adhesive dried completely, the stub was transferred into a sputter coater for gold coating under vacuum conditions. Finally, the gold-coated samples were carefully placed into the SEM chamber for morphological observation.

Experimental animal and treatment

The present study was approved by the Ethics Committee of Experimental Animals of The First Affiliated Hospital, Jiangxi Medical College, Nanchang University, and conducted in accordance with laboratory animal management and guidelines.

The male BALB/c mice, aged five weeks, were sourced from SPF Biotechnology Co., Ltd. in Beijing, China. The mice were raised in a typical environment, maintaining a temperature of 24 ± 2°C and humidity at 55 ± 10%, with a 12-hour light/dark cycle, ensuring ample access to both food and water. Subsequently, the mice were allocated randomly into three distinct groups ($n = 5$): the control group, the dextran sulfate sodium (DSS) group, and the DSS+CCM group. The mice in the control group were provided with regular water. A UC mouse model of UC was established by administering mice 3% DSS for 7 days (Dong et al. 2022). Specifically, the drinking water of mice was replaced with a 3% DSS solution, prepared at a volume of 5 ml *per* animal per day. The DSS solution was refreshed every two days (with the initial administration of DSS designated as Day 1, and subsequent refreshes occurring on Day 3 and Day 5). Following this, mice were administered a daily gavage of 70 mg/kg of empty chitosan microspheres, commencing on the day of model induction and continuing for seven consecutive days thereafter. Meanwhile, those in the DSS+CCM group received a similar daily gavage of 70 mg/kg CCM for the same duration after model induction. On the eighth day of the experiment, euthanasia of the mice was performed using a lethal dose of CO_2, after which their colonic tissues were harvested for subsequent histological examination and scRNA-seq analysis.

Assessment of disease activity index (DAI)

The body mass, hidden blood, and stool texture of all mice were meticulously documented on a daily basis. The average daily DAI score for each mouse was computed following the established protocol: weight reduction (0 score: <1%, 1 score: 1–5%, 2 score: 5–10%, 3 score: 10–15%, 4 score: 15–20%), hidden blood (0 score: negative, 2 score: positive, 4 score: visible), stool texture (0 score: normal, 2 score: soft, 4 score: liquid) (Camussi et al. 2015).

Hematoxylin and eosin (HE) staining

Colon tissue samples were harvested and preserved in a 4% buffered paraformaldehyde solution, subsequently subjected to a dehydration process utilizing a gradient of alcohol concentrations at 75%, 85%, 95%, and 100%. These specimens were then embedded in paraffin and underwent a dewaxing procedure with xylene. The processed tissues were sectioned into slices measuring 4 μm. Following this, the slices were stained with hematoxylin and eosin, and subsequently sealed with neutral gum. Optical microscopy (Olympus, CKX53) was employed to capture images of the prepared samples.

Immunofluorescence

Colon tissues were fixed in precooled 4% paraformaldehyde and blocked with 3% BSA. Sections embedded in paraffin were subjected to dewaxing using xylene, followed by rehydration through a gradient of alcohol concentrations (100%–95%–80%). Subsequently, the sections underwent antigen retrieval through a high-pressure treatment for 5 minutes in a citrate buffer at pH 6.0, and were permeabilized utilizing 0.5% Triton X-100, after which goat serum was introduced. The sections were then stained with an anti-NLRP12 antibody (1:500, sc-390666, Santa Cruz) and anti-ZO-1 antibody (1:100, 13663, CST), followed by successive incubation with a secondary antibody, goat anti-mouse Alexa Flour 488 (1:200, ab150117, Abcam), and an antifade mounting medium containing DAPI (C1006, Beyotime) for nuclear counterstaining. Ultimately, images were captured using an optical microscopy (Olympus, CKX53).

Cell culture and CCM treatment

Human colorectal adenocarcinoma cell line Caco2 cells were purchased from Procell (CL-0050), and the culture conditions are MEM basic medium containing 20% fetal bovine serum and 1% penicillin-streptomycin, incubated at 37°C in an environment with 5% CO_2. For establishing UC cell model, Caco2 cells were treated with 1 μg/ml lipopolysaccharide (LPS) for 3 hours and then incubated with 5 mM ATP for 30 min. Caco2 cells were treated with different doses of CCM (Ctrl, Ctrl + physiological saline, 10, 20, 40, 80 μM) to investigate the toxic effects of CCM on cells.

CCK8 analysis

Prepared a single cell suspension from the cells, and after counting, adjusted each group of cells to 2×10^4 cells/ml. Plated 100 μl of cells *per* well, which amounts to 1000 cells/well. Each sample group should have 6 replicates, and added 100 μl of sterile water or PBS to the edge wells. Treated the cells with different doses of CCM. Before detection, replaced the medium with 100 μl of fresh culture medium and added 10 μl of CCK-8 to each well. After 1 hour, measured the OD value at 450 nm using a microplate reader (Infinite M1000, TECAN).

Flow cytometry

Cells were centrifuged to pellet the cells and then genteelly washed with PBS to remove any residual culture medium or debris followed by washed with 200 μl Binding Buffer. Next, added 10 μl of propidium iodide (PI) to the cell suspension according to the manufacturer's instructions. Incubated the cells in the dark at room temperature for 10–15 min to allow binding of PI to DNA in permeabilized cells. After incubation, samples were detected using a flow cytometer (FACSVerse^{TM}, BD).

ELISA analysis

Level of interleukin 18 (IL-18) and IL-1β were detected by Human (IL-18) ELISA Kit (ml058055, mlbio) and Human interleukin 1β (IL-1β) ELISA Kit (ml058059, mlbio), according to the manufacturer's recommendations, respectively.

Western blot (WB)

Homogenize the tissue or lyse the cells using a RIPA lysis buffer containing protease inhibitors to prevent protein degradation. Protein quantification was measured using a BCA method. Equal amounts of protein were loaded onto the gel for 10% SDS-PAGE and then performed the transfer to PVDF membranes. Incubated the membranes in a 5% non-fat dry milk in TBST blocking buffer for 1–2 hours at room temperature with gentle shaking to prevent non-specific binding of antibodies or overnight at 4°C. Diluted the primary antibody, including ASC (1:10000, 10500-1-AP, Proteintech), NLRP3 (1:5000, 68102-1-lg, Proteintech), NLRP12 (1:1000, sc-390666, Santa Cruz), caspase-8 (1:5000, 66093-1-lg, Proteintech), GAPDH (1:15000, 60004-1-lg, Proteintech), in blocking buffer and then incubate the membranes overnight at 4°C with gentle shaking. After washing with TBST to remove unbound primary antibody, membranes were incubated with the secondary antibody Goat Anti-Mouse IgG H&L (HRP) (1:1000, ab205719, Abcam) and Goat Anti-Rabbit IgG H&L (HRP) (1:20000, ab6721, Abcam) for 1 hour at room temperature. High-sensitive ECL luminescence kit was used for color rendering, chemiluminescence imaging analysis system was used for exposure and pictures were collected.

Statistical analysis

The statistical analysis of the data was completed using GraphPad Prism 9.0 software. Comparisons between multiple groups were performed using ANOVA followed by Tukey's *post hoc* test. Statistical significance was considered when p was less than 0.05.

Results

CCM treatment alleviates DSS-induced UC in mice

The morphology and size distribution of CCM were evaluated by SEM. As shown in the representative SEM image (Fig. 1A), the microspheres exhibit a smooth, aggregated surface topology composed of numerous closely packed spherical nanoparticles. These particles display uniform dispersion and a relatively consistent size distribution, with approximately 100 nm diameters. Next, we established UC mice models induced by DSS and treated it with CCM to evaluate the therapeutic effect of CCM on UC mice (Fig. 1B). The results showed that the body weight of UC mice remained unchanged, but the colon length significantly decreased, and the DAI score and concentration of inflammatory factors of IL-18 and IL-1β significantly increased, compared to the Ctrl group (Fig. 1C–G). However, CCM treatment significantly inhibited the damage of DSS to the colon tissue of mice, as evidenced by the CCM increased colon length and decreased DAI score and concentration of inflammatory factors without affecting the body weight of the mice (Fig. 1C–G). The HE staining observed that CCM significantly reduced histology score and restored the mucosal damage, ulceration, and crypt loss caused by DSS (Fig. 1H–I), confirming the protective effect of CCM on the colon. Taken together, CCM treatment alleviates DSS-induced UC in mice.

CCM inhibits PANoptosis to alleviate DSS-induced UC in mice

To explore whether the improvement effect of CCM on UC mice is related to the PANoptosis of epithelial cells, we isolated the colon tissues of mice and performed double immunofluorescence staining for ZO-1 and NLRP12 (Fig. 2). Immunostaining of the tight junction marker ZO-1 was used to outline the morphology of intestine. NLRP12 immunostaining was used to assess the level of PANoptosis. The immunofluorescence results showed that ZO-1 was strongly

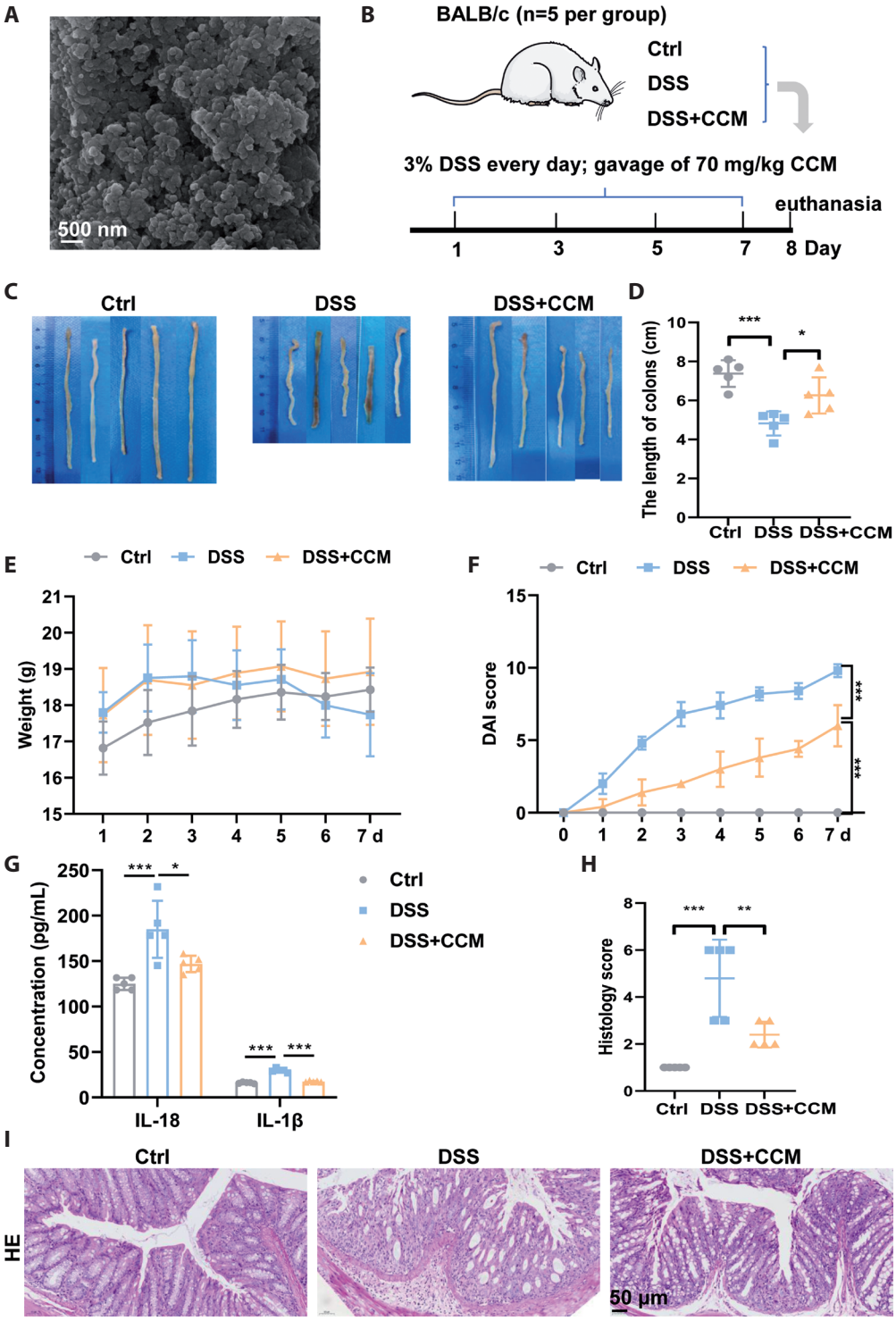

Figure 1. CCM treatment alleviates DSS-induced UC in mice. **A.** SEM images of CCM. Scare bar: 500 nm. **B.** Schematic diagram illustrating the experimental timeline of DSS-induced colitis model establishment and treatment with CCM in mice. **C.** Images of colonic tissues from three groups of mice. **D.** Statistical graph of colonic tissue lengths in three groups of mice. **E.** Weight statistics line graph of three groups of mice. **F.** DAI score statistics in three groups of mice. **G.** ELISA detection of IL-18 and IL-1β concentrations in colonic tissues of three groups of mice. **H.** Histopathological score statistics of colonic tissues in three groups of mice. **I.** Representative H&E stained images of colonic tissues from three groups of mice. Scare bar: 50 μm. Ctrl, blank control group; DSS, mice treated with DSS induction to establish UC model; DSS+CCM, mice treated with DSS induction to establish UC model and then gavaged with CCM. $n = 5$; * $p < 0.05$, ** $p < 0.01$, *** $p < 0.001$.

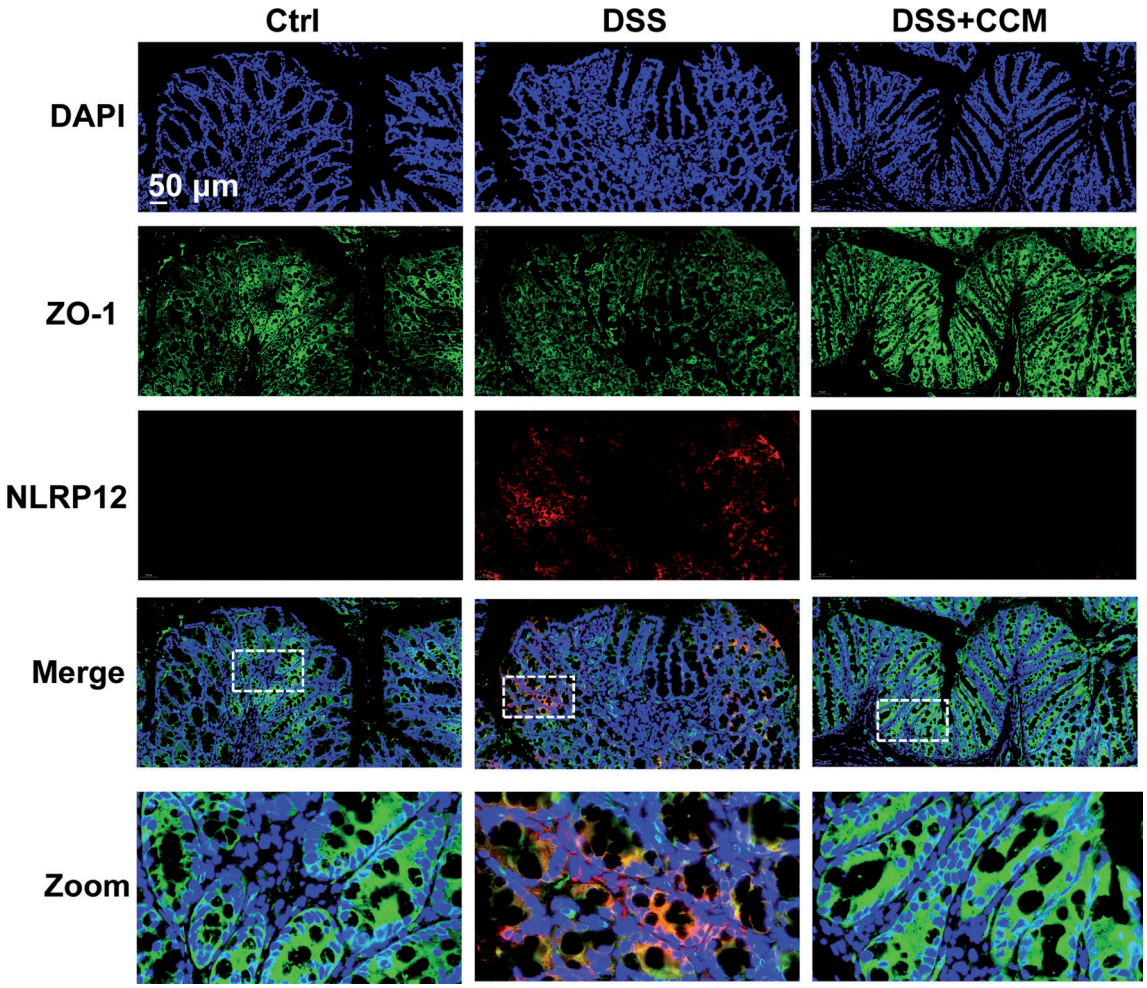

Figure 2. Double immunofluorescence staining for ZO-1 (green) and NLRP12 (red) of colonic tissue in three groups of mice. Scare bar: 50 μm. Ctrl, blank control group; DSS, mice treated with DSS induction to establish UC model; DSS+CCM, mice treated with DSS induction to establish UC model and then gavaged with CCM. NLRP12 expression upregulated by DSS induction.

expressed in all three groups of colon tissues, but the DSS group exhibited a slight decrease in ZO-1 expression due to glandular disarray and crypt loss. In contrast, there were significant intergroup differences in the expression of NLRP12 in colon tissues, with DSS induction leading to strong expression of NLRP12, while CCM treatment significantly inhibited this induction. Furthermore, NLRP12 and ZO-1 were co-localized in colon tissues. These results suggest that CCM can inhibit the PANoptosis to improve UC in mice.

scRNA-seq data reveals PANoptosis in intestinal epithelial cells

In our previous research, we conducted single-cell RNA sequencing on colon tissues from DSS mice treated or untreated with CCM (Fig. 3A). A total of 7 cell types were identified in the colon tissue, with epithelial cells exhibiting the highest PANoptosis score (Fig. 3A). Therefore, we focused on our epithelial cells. Here, we perform an in-depth analysis of epithelial cells in that data. Based on the expression of known marker genes, epithelial cells were annotated into eight subpopulations (Fig. 3B). The expression of the top five marker genes for each subpopulation is shown in a bubble chart (Fig. 3B). We then explored the levels of PANoptosis in different epithelial cell subpopulations. The results showed that the PANoptosis score in the crypt top colonocytes (CT) subpopulation was the highest (Fig. 3C). Furthermore, the PANoptosis score in the CT subpopulation of the CCM treatment group significantly decreased compared to the DSS group (Fig. 3D). Next, the expression of PANoptosis-related markers (PYCARD, NLRP3, NLRP12, and caspase-8) in epithelial cells was assessed. Among these four genes, the expression of NLRP3 and NLRP12 was very low in various subpopulations of epithelial cells, while PYCARD and cas-

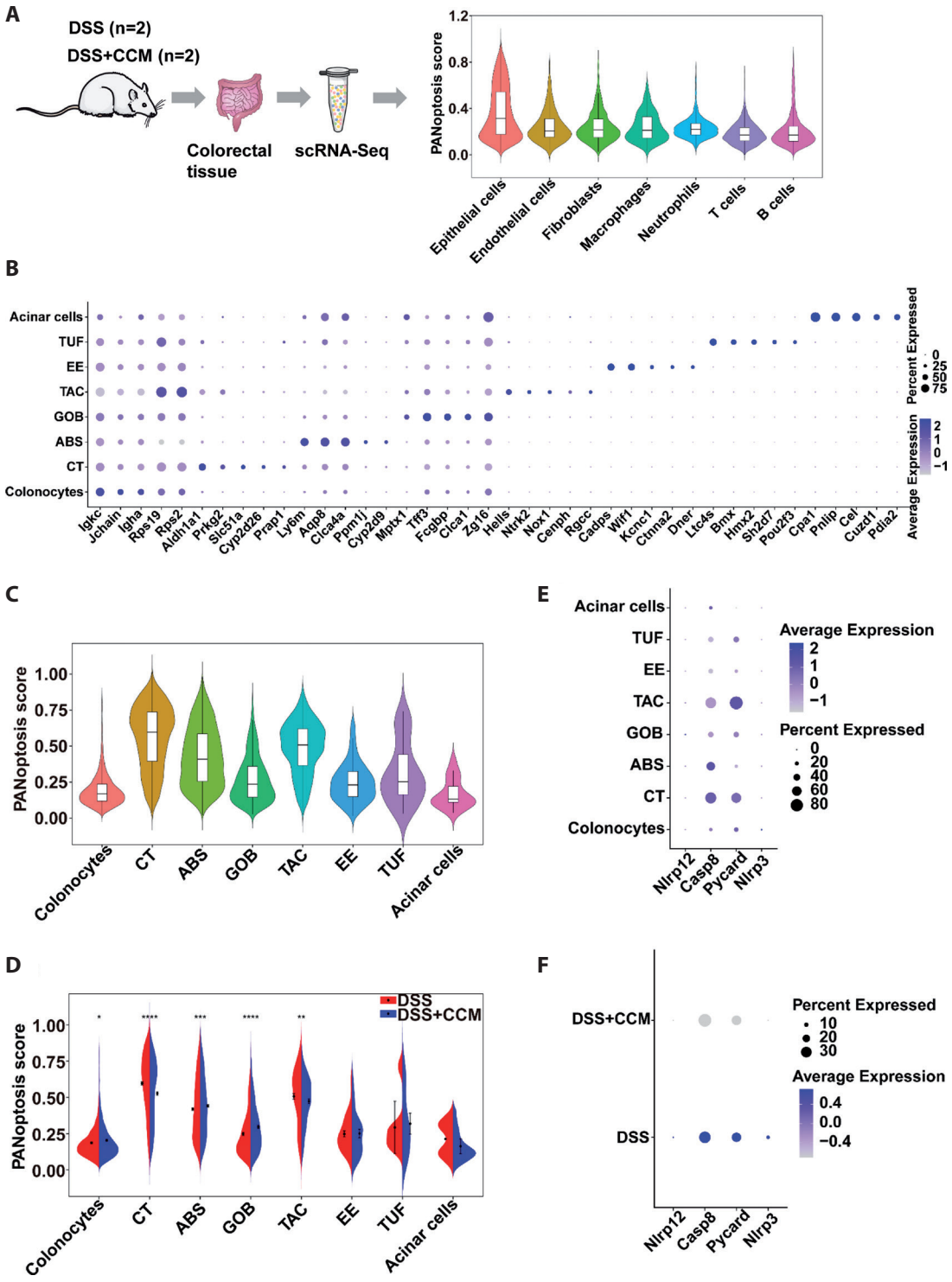

Figure 3. scRNA-seq data reveals PANoptosis in intestinal epithelial cells. **A.** Schematic diagram of the scRNA-seq workflow and violin plot of PANoptosis score in seven cell types. **B.** Bubble plot of top 5 markers of eight subtypes epithelial cells. **C.** Violin plot of PANoptosis score in eight subtypes epithelial cells. **D.** Violin plot of PANoptosis score in eight subtypes epithelial cells between two groups. **E.** Bubble plot of expression of PANoptosis-related genes (NLRP12, caspase-8, PYCARD, NLRP3) in eight subtypes epithelial cells. **F.** Bubble plot of expression of PANoptosis-related genes (NLRP12, caspase-8, PYCARD, NLRP3) in two groups. DSS, mice treated with DSS induction to establish UC model; DSS+CCM, mice treated with DSS induction to establish UC model and then gavaged with CCM; CT, crypt top colonocytes; TAC, transit amplifing cells; EE, enteroendocrine cell; GOB, Goblet cell; ABS, absorptive cell; TUF, tuft cell. * $p < 0.05$, ** $p < 0.01$, *** $p < 0.001$.

pase-8 were mainly highly expressed in the CT and transit amplifying cells (TAC) subpopulations (Fig. 3E). We also observed that these four proteins were down-regulated in colon tissues after CCM treatment relative to the DSS group (Fig. 3F). These results suggest that CCM treatment for UC may be related to the inhibition of epithelial cell PANoptosis.

CCM ameliorate cellular inflammation in vitro by inhibiting PANoptosis

Subsequently, the regulatory effects of CCM on inflammation and PANoptosis in intestinal epithelial cells were investigated *in vitro*. Initially, the cytotoxicity of CCM on Caco-2 cells was assessed using the CCK8 assay. The results showed that the viability of Caco-2 cells remained unchanged, or even slightly increased, with increasing concentrations of CCM, indicating that CCM has no toxic effect on Caco-2 cells (Fig. 4A). Therefore, in subsequent studies, Caco-2 cells were treated with three different concentrations of CCM (20, 40, 80 μM). The results of the ELISA show that the abundance of IL-18 and IL-1β in Caco-2 cells significantly enhanced after LPS induction, but this upregulation was significantly reversed by CCM treatment (Fig. 4B). Flow cytometry results revealed that, compared to the blank control group, LPS induction

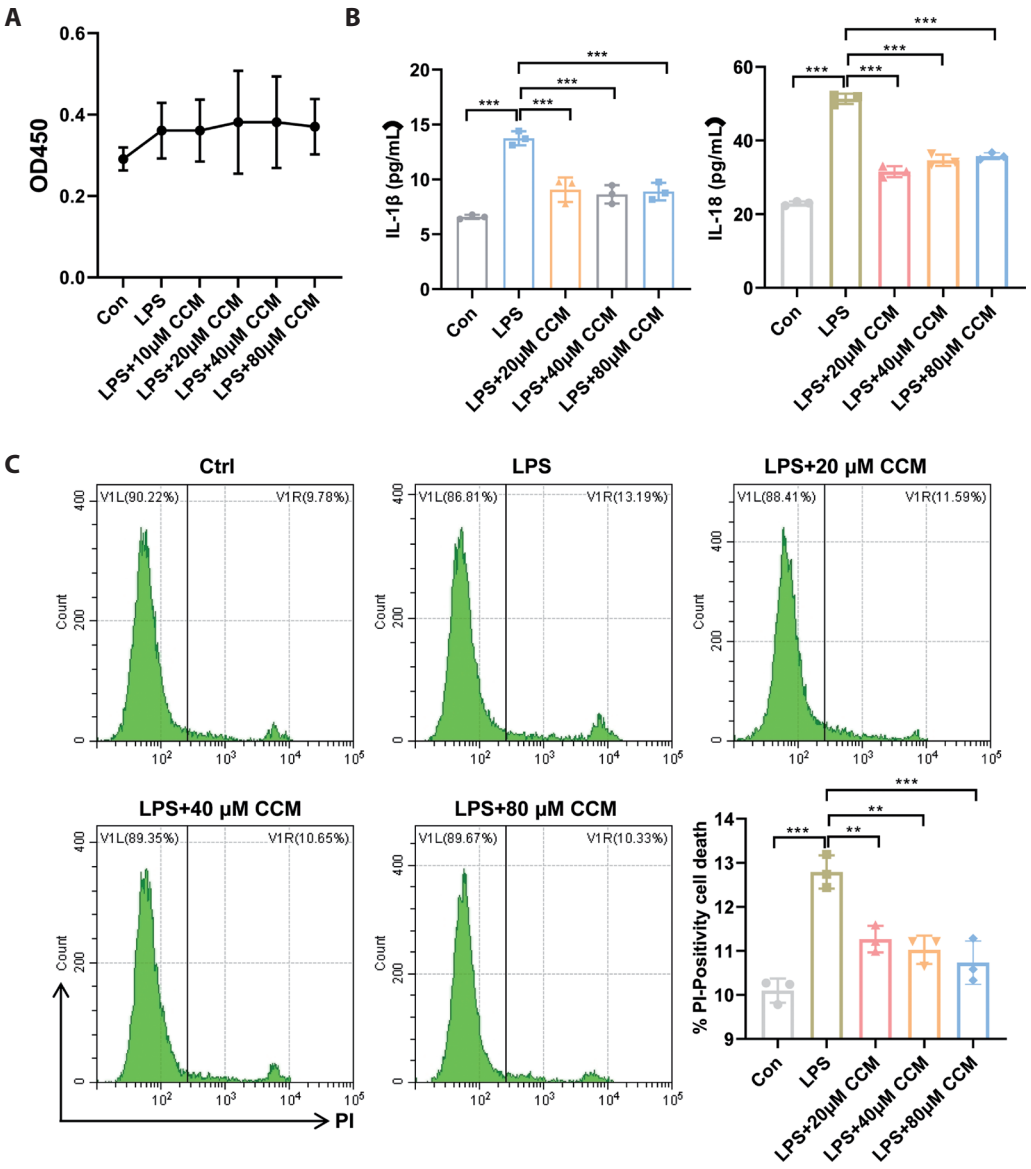

Figure 4. CCM ameliorate cellular inflammation *in vitro*. **A.** The viability of Caco-2 cells was detected by CCK8 assay. **B.** The abundance of IL-18 and IL-1β in Caco-2 cells was detected by ELISA. **C.** Cell death of Caco-2 cells was detected by flow cytometry. Caco-2 cells were treated with different concentrations of CCM (20, 40, 80 μM). $n = 3$, ** $p < 0.01$, *** $p < 0.001$.

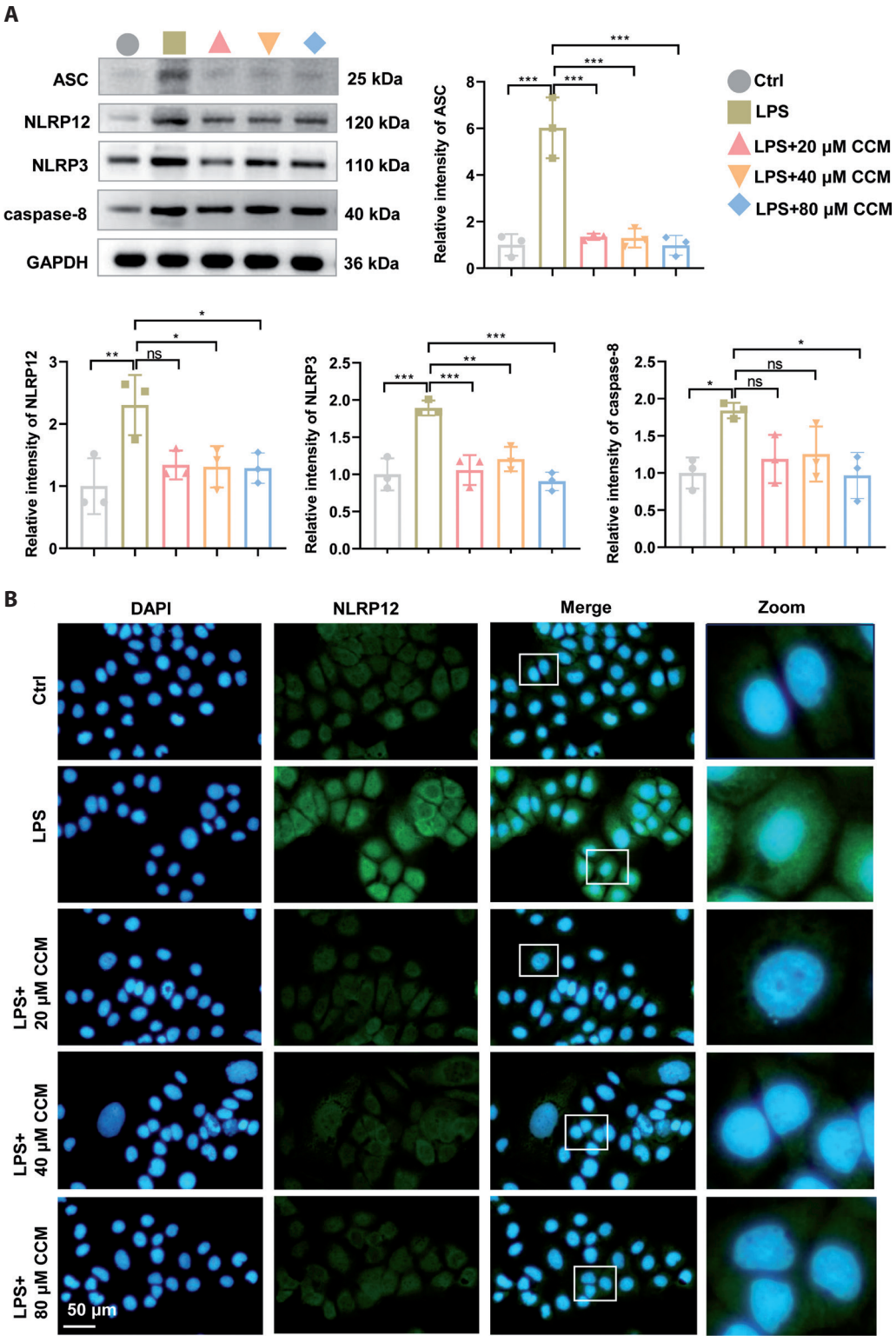

Figure 5. CCM ameliorate cellular inflammation *in vitro* by inhibiting PANoptosis. **A.** The protein expression of PANoptosis-related proteins (ASC, NLRP3, NLRP12, and caspase-8) of Caco-2 cells was detected by WB. **B.** Immunofluorescence staining of NLRP12 of Caco-2 cells. Caco-2 cells were treated with different concentrations of CCM (20, 40, 80 μM). $n = 3$, $^{ns}\ p > 0.05$, $^{*}\ p < 0.05$, $^{**}\ p < 0.01$, $^{***}\ p < 0.001$.

significantly boosted cell apoptosis, while all three concentrations of CCM significantly reduced the LPS-induced increase in cell death (Fig. 4C). These results indicated that CCM exhibits a protective effect on Caco-2 cells *in vitro*. We next used WB to detect the expression of PANoptosis-related proteins (ASC, NLRP3, NLRP12, and caspase-8) to assess the effect of CCM on LPS-induced PANoptosis in Caco-2 cells. As shown in Figure 5A, under the inflammatory context induced by LPS, the expression of PANoptosis-related proteins in Caco-2 cells was significantly potentiated. However, CCM treatment resulted in a significant decrease in the expression of these proteins compared to the LPS group, particularly at the 80 μM dose. Immunofluorescence staining of NLRP12 further supported the results from WB, as reflected by CCM reversed the provoking in NLRP12 expression caused by LPS induction (Fig. 5B). These results suggest that CCM can inhibit PANoptosis in Caco-2 cells *in vitro*.

Discussion

In 2023, the global prevalence of UC was estimated to be 5 million cases, with an increasing incidence rate worldwide (Le Berre et al. 2023). Given the high incidence in developed countries and the significant rise in developing countries, UC has evolved into a global burden. The search for safe and effective preventive and therapeutic agents for UC is an urgent clinical issue. In this study, we demonstrated that CCM significantly suppress UC inflammation and PANoptosis of intestinal epithelial cells both *in vitro* and *in vivo*. This provides a theoretical basis and practical support for the protective effects of CCM on UC, offering a clearer direction and target for its implementation.

Curcumin, a phenolic compound extracted from the rhizome of the plant Curcuma longa (turmeric), possesses a wide range of pharmacological properties, including anti-inflammatory, antioxidant, lipid-lowering, anticoagulant, anticancer, and free radical scavenging activities (Marton et al. 2022). Curcumin alleviates DSS-induced colitis by modulating M1/M2 macrophage polarization and Toll-like receptor (TLR) signaling pathways (Kang et al. 2021). Gong et al. (2018) found that curcumin mitigates DSS-induced colitis by inhibiting NLRP3 inflammasome activation and IL-1β production. Our research team also confirmed during the screening of therapeutic agents for UC that curcumin exhibits significant anti-UC effects, markedly improving colonic mucosal damage in UC rats, suggesting its potential application value in UC prevention and treatment (Huang et al. 2017). However, we also observed that curcumin has poor stability, low water solubility under acidic and neutral conditions, rapid decomposition under alkaline conditions, and a short *in vivo* metabolic half-life, which severely limits its use as a drug formulation. Therefore, we employed chitosan as a carrier for curcumin. Chitosan is a polymer with multiple biological characteristics, such as harmlessness, biodegradability, and viscosity, and its biocompatibility makes it an ideal carrier for sustained drug release, enhancing drug bioavailability (Peers et al. 2020). Chitosan microspheres have significant applications in drug delivery systems. Saranya et al. prepared curcumin-chitosan microspheres and found that they exhibit good antibacterial, antioxidant, and anti-inflammatory activities (Saranya et al. 2018; Pramanik and Sali 2021). Furthermore, a recent study has emphasized the critical role of delivery systems in enhancing the functional performance of bioactive compounds. Zhang et al. (2024) reviewed the use of egg white protein (EWP)-based delivery vehicles and demonstrated that biopolymer assemblies at various scales can effectively stabilize unstable nutraceuticals such as curcumin, thereby improving their bioavailability and bioefficacy. These delivery systems often assembled with or without auxiliary components like polysaccharides or polyphenols, were shown to protect labile compounds against degradation and promote their functional performance in complex food and physiological environments. Importantly, it is worth noting that in our previously published study, we directly compared the therapeutic effects of free curcumin and CCM in DSS-induced colitis mice (Yu et al. 2022). The results demonstrated that CCM significantly outperformed free curcumin in reducing inflammatory. In this context, it is reasonable to infer that the CCM used in our study might also confer such stabilization and delivery advantages. Indeed, we confirmed that CCM significantly improve pathological damage in UC mice. Nevertheless, more evidence is still needed for the preclinical use of CCM.

Curcumin has been shown to exert its effects through multiple mechanisms, including the regulation of mitochondrial pathways, and the activation of PANoptosis. For example, curcumin-activated mesenchymal stem cells derived from olfactory mucosa alleviate neuronal PANoptosis through the modulation of microglial polarization in cerebral ischemia/reperfusion injury (Lan et al. 2024). Curcumin exerts a protective role of against PANoptosis of corneal endothelial cells and the adhesion of monocytes triggered by tumor necrosis factor-alpha and interferon-gamma in rats (Guo et al. 2024). Furthermore, there is existing fewer evidence supporting the role of PANoptosis in mediating the pathological progression of UC, for instance, ZBP1-dependent PANoptosis was observed in DSS-induced UC mice (Ye et al. 2024). Five PANoptosis-related genes (ZBP1, AIM2, CASP1/8, IRF1) are abnormal expressed in UC patients (Wang et al. 2023), another seven PANoptosis-related genes (IL6, CASP1, ABCB1, ANXA5, PPARG, NOS2, and TGM2) not only exhibit abnormal expression but also form a predictive model capable of diagnosing UC patients (Ji et al. 2024), and additional PANoptosis-related genes (TIMP1, TIMP2, TIMP3, IL6, and CCL2) also have strong diagnostic

performance (Lu et al. 2024). These studies collectively underscore the significant role of PANoptosis in UC. However, whether CCM can protect the intestine from UC-induced damage through PANoptosis remains unreported. This study is the first to demonstrate that the protective effect of CCM against UC is mediated by inhibiting PANoptosis in intestinal epithelial cells.

Conclusion

In summary, this study has demonstrated both *in vitro* and *in vivo* that the therapeutic efficacy of CCM in UC mice is exerted through the inhibition of PANoptosis in intestinal epithelial cells. Notably, our findings reveal for the first time that PANoptosis plays a critical role in UC pathogenesis, and that its suppression is a novel mechanism underlying the protective effect of CCM. This mechanistic insight not only expands the current understanding of UC pathology but also provides a promising foundation for the development of CCM as a clinically applicable therapeutic agent.

Author contributions. XP: Conceptualization, Investigation, and Writing – original draft; QZ, YX: Investigation and Writing – original draft; JL: Investigation and Validation; FZ: Investigation, Data curation and Writing – review & editing; GH: Methodology, Supervision and Writing – review & editing. All authors read and approved the final version of the manuscript.

Conflict of interest. The authors declared that they have no conflict of interest.

Acknowledgements. This study was supported by the Regional Science Fund project (82260807).

Ethics approval. The present study was approved by the Ethics Committee of Experimental Animals of The First Affiliated Hospital, Jiangxi Medical College, Nanchang University, and conducted in accordance with laboratory animal management and guidelines.

Data availability. The datasets used and/or analyzed during the current study are available from the corresponding author on reasonable request.

References

Ben-Horin S, Salomon N, Karampekos G, Viazis N, Lahat A, Ungar B, Eliakim R, Kuperstein R, Kriger-Sharabi O, Reiss-Mintz H, et al. (2024): Curcumin-QingDai combination for patients with active ulcerative colitis: A Randomized, double-blinded, placebo-controlled trial. Clin. Gastroenterol. Hepatol. **22,** 347-356 https://doi.org/10.1016/j.cgh.2023.05.023

Camussi G, Yang J, Liu X-X, Fan H, Tang Q, Shou Z-X, Zuo D-M, Zou Z, Xu M, Chen Q-Y, et al. (2015): Extracellular vesicles derived from bone marrow mesenchymal stem cells protect against experimental colitis via attenuating colon inflammation, oxidative stress and apoptosis. Plos One **10,** e0140551 https://doi.org/10.1371/journal.pone.0140551

Dong Y, Fan H, Zhang Z, Jiang F, Li M, Zhou H, Guo W, Zhang Z, Kang Z, Gui Y, et al. (2022): Berberine ameliorates DSS-induced intestinal mucosal barrier dysfunction through microbiota-dependence and Wnt/β-catenin pathway. Int. J. Biol. Sci. **18,** 1381-1397 https://doi.org/10.7150/ijbs.65476

Feng J, Wang Z, Huang W, Zhao X, Xu L, Teng C, Li Y (2025a): Hyaluronic acid-decorated lipid nanocarriers as novel vehicles for curcumin: Improved stability, cellular absorption, and anti-inflammatory effects. Food Chem. **463,** 141420 https://doi.org/10.1016/j.foodchem.2024.141420

Feng J, Wang Z, Zhao X, Xu L, Teng C, Liu S, Huang W, Li Y (2025b): Advanced targeted curcumin delivery using biodegradable hierarchical microspheres with calcium pectinate matrix and hyaluronic acid moieties for enhancing colitis amelioration. Carbohydr. Polym. **353,** 123273 https://doi.org/10.1016/j.carbpol.2025.123273

Feuerstein JD, Moss AC, Farraye FA (2019): Ulcerative Colitis. Mayo Clin. Proc. **94,** 1357-1373 https://doi.org/10.1016/j.mayocp.2019.01.018

Gong Z, Zhao S, Zhou J, Yan J, Wang L, Du X, Li H, Chen Y, Cai W, Wu J (2018): Curcumin alleviates DSS-induced colitis via inhibiting NLRP3 inflammsome activation and IL-1beta production. Mol. Immunol. **104,** 11-19 https://doi.org/10.1016/j.molimm.2018.09.004

Guo R, Yu Y, Xu C, Ma M, Hou C, Dong X, Wu J, Ouyang C, Ling J, Huang T (2024): Protective effects of curcumin on corneal endothelial cell PANoptosis and monocyte adhesion induced by tumor necrosis factor-alpha and interferon-gamma in rats. Exp. Eye Res. **245,** 109952 https://doi.org/10.1016/j.exer.2024.109952

Huang G, Ye L, Du G, Huang Y, Wu Y, Ge S, Yang Z, Zhu G (2017): Effects of curcumin plus Soy oligosaccharides on intestinal flora of rats with ulcerative colitis. Cell Mol. Biol. **63,** 20-25 https://doi.org/10.14715/cmb/2017.63.7.3

Huang G, Ye L, Du G, Huang Y, Wu Y, Ge S, Yang Z, Zhu G (2017): Effects of curcumin plus Soy oligosaccharides on intestinal flora of rats with ulcerative colitis. Cell Mol. Biol. **63,** 20-25 https://doi.org/10.14715/cmb/2017.63.7.3

Ji Y, Li P, Ning T, Yang D, Shi H, Dong X, Zhu S, Li P, Zhang S (2024): PANoptosis-related genes: Molecular insights into immune dysregulation in ulcerative colitis. J. Gastroenterol. Hepatol. **40,** 177-191 https://doi.org/10.1111/jgh.16804

Kang ZP, Wang MX, Wu TT, Liu DY, Wang HY, Long J, Zhao HM, Zhong YB (2021): Curcumin alleviated dextran sulfate sodium-induced colitis by regulating M1/M2 macrophage polarization and TLRs signaling pathway. Evid. Based. Complement. Alternat. Med. **2021,** 3334994 https://doi.org/10.1155/2021/3334994

Lan Z, Tan F, He J, Liu J, Lu M, Hu Z, Zhuo Y, Liu J, Tang X, Jiang Z, et al. (2024): Curcumin-primed olfactory mucosa-derived mesenchymal stem cells mitigate cerebral ischemia/reperfusion injury-induced neuronal PANoptosis by modulating microglial polarization. Phytomedicine **129,** 155635

https://doi.org/10.1016/j.phymed.2024.155635
Le Berre C, Honap S, Peyrin-Biroulet L (2023): Ulcerative colitis. Lancet **402,** 571-584
https://doi.org/10.1016/S0140-6736(23)00966-2
Lu J, Li F, Ye M (2024): PANoptosis and autophagy-related molecular signature and immune landscape in ulcerative colitis: Integrated analysis and experimental validation. J. Inflamm. Res. **17,** 3225-3245
https://doi.org/10.2147/JIR.S455862
Marton LT, Barbalho SM, Sloan KP, Sloan LA, Goulart RA, Araujo AC, Bechara MD (2022): Curcumin, autoimmune and inflammatory diseases: going beyond conventional therapy – a systematic review. Crit. Rev. Food Sci. Nutr. **62,** 2140-2157
https://doi.org/10.1080/10408398.2020.1850417
Molodecky NA, Soon IS, Rabi DM, Ghali WA, Ferris M, Chernoff G, Benchimol EI, Panaccione R, Ghosh S, Barkema HW, et al. (2012): Increasing incidence and prevalence of the inflammatory bowel diseases with time, based on systematic review. Gastroenterology **142,** 46-54
https://doi.org/10.1053/j.gastro.2011.10.001
Nelson KM, Dahlin JL, Bisson J, Graham J, Pauli GF, Walters MA (2017): The essential medicinal chemistry of curcumin. J. Med. Chem. **60,** 1620-1637
https://doi.org/10.1021/acs.jmedchem.6b00975
Peers S, Montembault A, Ladaviere C (2020): Chitosan hydrogels for sustained drug delivery. J. Control. Release **326,** 150-163
https://doi.org/10.1016/j.jconrel.2020.06.012
Pramanik S, Sali V (2021): Connecting the dots in drug delivery: A tour d'horizon of chitosan-based nanocarriers system. Int. J. Biol. Macromol. **169,** 103-121
https://doi.org/10.1016/j.ijbiomac.2020.12.083
Saranya TS, Rajan VK, Biswas R, Jayakumar R, Sathianarayanan S (2018): Synthesis, characterisation and biomedical applications of curcumin conjugated chitosan microspheres. Int. J. Biol. Macromol. **110,** 227-233
https://doi.org/10.1016/j.ijbiomac.2017.12.044
Sun X, Yang Y, Meng X, Li J, Liu X, Liu H (2024): PANoptosis: Mechanisms, biology, and role in disease. Immunol. Rev. **321,** 246-262
https://doi.org/10.1111/imr.13279
Wang JM, Yang J, Xia WY, Wang YM, Zhu YB, Huang Q, Feng T, Xie LS, Li SH, Liu SQ, et al. (2023): Comprehensive analysis of PANoptosis-related gene signature of ulcerative colitis. Int. J. Mol. Sci. **25,** 348
https://doi.org/10.3390/ijms25010348
Xu L, He B, Sun Y, Li J, Shen P, Hu L, Liu G, Wang J, Duan L, Zhan S, et al. (2023): Incidence of inflammatory bowel disease in urban China: A Nationwide population-based study. Clin. Gastroenterol. Hepatol. **21,** 3379-3386
https://doi.org/10.1016/j.cgh.2023.08.013
Yao H, Wang F, Chong H, Wang J, Bai Y, Du M, Yuan X, Yang X, Wu M, Li Y, et al. (2023): A Curcumin-modified coordination polymers with ROS scavenging and macrophage phenotype regulating properties for efficient ulcerative colitis treatment. Adv. Sci. **10,** e2300601
https://doi.org/10.1002/advs.202300601
Ye Z, Deng M, Yang Y, Song Y, Weng L, Qi W, Ding P, Huang Y, Yu C, Wang Y, et al. (2024): Epithelial mitochondrial fission-mediated PANoptosis is crucial for ulcerative colitis and its inhibition by saquinavir through Drp1. Pharmacol. Res. **210,** 107538
https://doi.org/10.1016/j.phrs.2024.107538
Yu S, Huang Y, Huang G, Xiong J, Wu Y, Lei X (2019): Effects of curcumin chitosan microspheres on the expression of NF-κB, IL-1β, IL-4 and IL-6 in rats with ulcerative colitis. J. Biomater. Tissue Eng. **9,** 810-815
https://doi.org/10.1166/jbt.2019.2053
Yu S, Huang Y, Wu Y, Wu Y, Huang G, Xiong J, You YJFS, Technology (2022): Curcumin chitosan microsphere improve ulcerative colitis inflammatory response by regulating miR-224-3p/TLR4 axise. Food Sci. Technol. **42,** e65721
https://doi.org/10.1590/fst.65721
Yuan H, Zhou L, Chen Y, You J, Hu H, Li Y, Huang R, Wu S (2023): Salmonella effector SopF regulates PANoptosis of intestinal epithelial cells to aggravate systemic infection. Gut Microbes **15,** 2180315
https://doi.org/10.1080/19490976.2023.2180315
Zhang H, Shi X, Li Y, Li S, Zhang L, Huang X, Yang M, Du Z, Liu J, Zhang T (2024): Enhancing the stability and biological activity of curcumin through incorporating zein-sodium alginate-egg white peptides hybrid assemblies. Food Bioscience **59,** 103868
https://doi.org/10.1016/j.fbio.2024.103868

Received: February 6, 2025
Final version accepted: June 27, 2025